

2019

(p)ppGpp and CodY promote *Enterococcus faecalis* virulence in a murine model of catheter-associated urinary tract infection

C. Colomer-Winter
University of Florida

A. L. Flores-Mireles
Washington University School of Medicine in St. Louis

S. Kundra
University of Florida

S. J. Hultgren
Washington University School of Medicine in St. Louis

J. A. Lemos
University of Florida

Follow this and additional works at: https://digitalcommons.wustl.edu/open_access_pubs

Recommended Citation

Colomer-Winter, C.; Flores-Mireles, A. L.; Kundra, S.; Hultgren, S. J.; and Lemos, J. A., "(p)ppGpp and CodY promote *Enterococcus faecalis* virulence in a murine model of catheter-associated urinary tract infection." *mSphere*, . . (2019).
https://digitalcommons.wustl.edu/open_access_pubs/8045

(p)ppGpp and CodY Promote *Enterococcus faecalis* Virulence in a Murine Model of Catheter-Associated Urinary Tract Infection

C. Colomer-Winter,^a A. L. Flores-Mireles,^{b,c*} S. Kundra,^a S. J. Hultgren,^{b,c} J. A. Lemos^a

^aDepartment of Oral Biology, University of Florida College of Dentistry, Gainesville, Florida, USA

^bDepartment of Molecular Microbiology, Washington University School of Medicine, St. Louis, Missouri, USA

^cCenter for Women's Infectious Disease Research, Washington University School of Medicine, St. Louis, Missouri, USA

ABSTRACT In *Firmicutes*, the nutrient-sensing regulators (p)ppGpp, the effector molecule of the stringent response, and CodY work in tandem to maintain bacterial fitness during infection. Here, we tested (p)ppGpp and *codY* mutant strains of *Enterococcus faecalis* in a catheter-associated urinary tract infection (CAUTI) mouse model and used global transcriptional analysis to investigate the relationship of (p)ppGpp and CodY. The absence of (p)ppGpp or single inactivation of *codY* led to lower bacterial loads in catheterized bladders and diminished biofilm formation on fibrinogen-coated surfaces under *in vitro* and *in vivo* conditions. Single inactivation of the bifunctional (p)ppGpp synthetase/hydrolase *rel* did not affect virulence, supporting previous evidence that the association of (p)ppGpp with enterococcal virulence is not dependent on the activation of the stringent response. Inactivation of *codY* in the (p)ppGpp⁰ strain restored *E. faecalis* virulence in the CAUTI model as well as the ability to form biofilms *in vitro*. Transcriptome analysis revealed that inactivation of *codY* restores, for the most part, the dysregulated metabolism of (p)ppGpp⁰ cells. While a clear linkage between (p)ppGpp and CodY with expression of virulence factors could not be established, targeted transcriptional analysis indicates that a possible association between (p)ppGpp and c-di-AMP signaling pathways in response to the conditions found in the bladder may play a role in enterococcal CAUTI. Collectively, data from this study identify the (p)ppGpp-CodY network as an important contributor to enterococcal virulence in catheterized mouse bladder and support that basal (p)ppGpp pools and CodY promote virulence through maintenance of a balanced metabolism under adverse conditions.

IMPORTANCE Catheter-associated urinary tract infections (CAUTIs) are one of the most frequent types of infection found in the hospital setting that can develop into serious and potentially fatal bloodstream infections. One of the infectious agents that frequently causes complicated CAUTI is the bacterium *Enterococcus faecalis*, a leading cause of hospital-acquired infections that are often difficult to treat due to the exceptional multidrug resistance of some isolates. Understanding the mechanisms by which *E. faecalis* causes CAUTI will aid in the discovery of new druggable targets to treat these infections. In this study, we report the importance of two nutrient-sensing bacterial regulators, named (p)ppGpp and CodY, for the ability of *E. faecalis* to infect the catheterized bladder of mice.

KEYWORDS (p)ppGpp, CAUTI, CodY, *Enterococcus*, stringent response

Catheter-associated urinary tract infections (CAUTIs) are one of the most common hospital-acquired infections, accounting worldwide for about 40% of all nosocomial infections (1–3). In addition to substantially increasing hospitalization time and costs, CAUTI can lead to serious and potentially deadly secondary bloodstream infections (4). Complicated CAUTI is often the result of bacteria forming biofilms on


Citation Colomer-Winter C, Flores-Mireles AL, Kundra S, Hultgren SJ, Lemos JA. 2019. (p)ppGpp and CodY promote *Enterococcus faecalis* virulence in a murine model of catheter-associated urinary tract infection. mSphere 4:e00392-19. <https://doi.org/10.1128/mSphere.00392-19>.

Editor Paul Dunman, University of Rochester

Copyright © 2019 Colomer-Winter et al. This is an open-access article distributed under the terms of the [Creative Commons Attribution 4.0 International license](https://creativecommons.org/licenses/by/4.0/).

Address correspondence to J. A. Lemos, jlemos@dental.ufl.edu.

* Present address: A. L. Flores-Mireles, Department of Biological Sciences, University of Notre Dame, Notre Dame, Indiana, USA. C.C.-W. and A.L.F.-M. contributed equally to the work.

 (p)ppGpp and CodY promote enterococcal CAUTI. @josealemos

Received 30 May 2019

Accepted 10 July 2019

Published 24 July 2019

indwelling urinary catheters, and enterococci (mainly *Enterococcus faecalis* and *Enterococcus faecium*) appear as the second leading cause of complicated CAUTI in many health care facilities (4–6). In addition, *E. faecalis* and *E. faecium* are major etiological agents of other life-threatening infections, such as infective endocarditis, and an even more serious threat to public health due to their exceptional antibiotic resistance (7). The recent rise in the number of enterococcal infections urges the development of new therapies, and understanding the mechanisms that promote *E. faecalis* CAUTI might uncover new druggable targets.

The pathogenic potential of *E. faecalis*, and of all enterococci in general, is tightly associated with its outstanding ability to survive an array of physical and chemical stresses, including common detergents and antiseptics; fluctuations in temperature, pH, and humidity; and prolonged starvation (7). The regulatory second messengers ppGpp (guanosine tetraphosphate) and pppGpp (guanosine pentaphosphate), collectively known as (p)ppGpp, broadly promote bacterial stress tolerance and virulence (8, 9). In *E. faecalis*, (p)ppGpp has been shown to promote virulence in invertebrate and vertebrate animal models and to mediate the expression of virulence-related traits such as growth in blood and serum, biofilm formation, intraphagocytic survival, and antibiotic tolerance (10–17). Originally described as the mediator of the stringent response (SR) (8), (p)ppGpp has distinct effects on bacterial physiology: at low (basal) concentrations, it fine-tunes bacterial metabolism to adjust cellular growth in response to mild environmental changes (18), whereas at high levels, it activates the SR responsible for promoting cell survival by slowing down growth-associated pathways and activating stress survival pathways (8, 18).

Two enzymes, the bifunctional synthetase/hydrolase Rel and the small alarmone synthetase RelQ, are responsible for enterococcal (p)ppGpp turnover (10, 19). Despite both Δrel and $\Delta rel \Delta relQ$ strains being unable to mount the SR (10, 13), there are fundamental differences in basal (p)ppGpp levels between these two strains. Specifically, while the double mutant, here called the (p)ppGpp⁰ strain, is completely unable to synthesize (p)ppGpp, basal (p)ppGpp levels are about 4-fold higher in the Δrel strain due to the constitutive and weak synthetase activity of RelQ (10, 14, 19). Accumulated evidence indicates that the metabolic control exerted by basal (p)ppGpp pools is more important during enterococcal infections than the semidormancy state characteristic of the SR (10, 13–17). This is exemplified by the distinct virulence phenotypes of Δrel and (p)ppGpp⁰ strains, both of which are unable to mount the SR. Specifically, while only the (p)ppGpp⁰ strain displayed attenuated virulence in *Caenorhabditis elegans* (10), *Galleria mellonella* (11, 13, 16), and a rabbit abscess model (15), the Δrel single mutant strain showed attenuated virulence in a rabbit model of infective endocarditis (17).

In low-GC Gram-positive bacteria such as *E. faecalis*, (p)ppGpp controls the transcription of nutrient uptake and amino acid biosynthesis genes via the branched-chain-amino-acid (BCAA)- and GTP-sensing CodY regulator (20). It follows that (p)ppGpp accumulation during BCAA starvation severely depletes intracellular GTP pools in all *Firmicutes* such that CodY regulation is severely impaired due to the depletion of its two cofactors (20). We recently confirmed the existence of the (p)ppGpp-CodY network in *E. faecalis* and demonstrated that inactivation of *codY* restored several phenotypes of the (p)ppGpp⁰ mutant strain, including virulence in *G. mellonella* (16). However, the contribution of the global nutritional regulator CodY to enterococcal pathogenesis in mammalian hosts remains unknown.

In this work, we examined the contribution of (p)ppGpp and CodY to the pathogenesis of *E. faecalis* in a murine CAUTI model (21). We discovered that, separately, basal levels of (p)ppGpp and the transcriptional regulator CodY promote biofilm formation in urine under *in vitro* conditions as well as virulence in a murine CAUTI model. Global transcriptome analysis validates previous findings that deletion of *codY* restores, at least in part, the dysregulated metabolism of the cell in the absence of (p)ppGpp. Finally, targeted mRNA quantifications reveal that the (p)ppGpp-CodY network alters the expression of genes coding for cyclic di-AMP (c-di-AMP) biosynthetic enzymes and of CAUTI virulence factors. Altogether, data from this study identify the

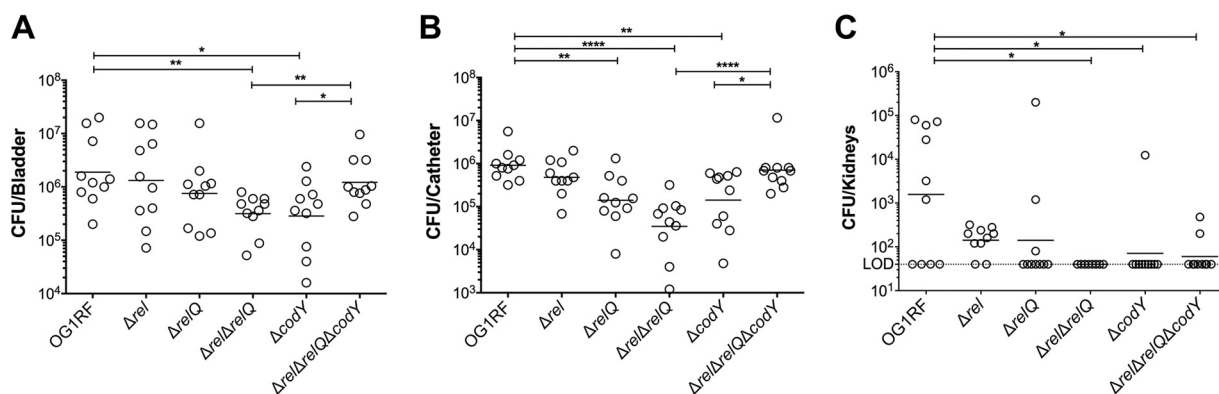


FIG 1 (p)ppGpp and CodY promote virulence of *E. faecalis* in a murine CAUTI model. The parent strain OG1RF and its derivatives were inoculated into the bladders of mice immediately after catheter implantation ($n = 10$). After 72 h, animals were euthanized, and bacterial burdens in bladders (A), catheters (B), and kidneys (C) were quantified. Graphs show total CFU recovered from these sites, each symbol represents an individual mouse, and the median value is shown as a horizontal line. Symbols on the dashed line indicate that recovery was below the limit of detection (LOD) (40 CFU). The data were pooled from two independent experiments. Two-tailed Mann-Whitney U tests were performed to determine significance (*, $P < 0.05$; **, $P < 0.005$; ***, $P < 0.0001$).

(p)ppGpp-CodY network as a contributor to enterococcal catheter colonization in the urinary tract and further support that basal levels of (p)ppGpp promote bacterial virulence through maintenance of a balanced bacterial metabolism.

RESULTS

The (p)ppGpp⁰ and $\Delta codY$ strains show impaired colonization in a murine CAUTI model. We compared the abilities of the *E. faecalis* OG1RF parent, Δrel , $\Delta relQ$, (p)ppGpp⁰, $\Delta codY$, and (p)ppGpp⁰ $\Delta codY$ strains to colonize and persist in the bladder of catheterized mice. Briefly, catheters were implanted into the bladders of C57BL/6Ncr mice prior to transurethral inoculation with $\sim 2 \times 10^7$ CFU of each designated strain. At 3 days postinfection, the OG1RF strain was readily recovered from bladders (6.3 ± 0.6 log₁₀ CFU) and catheters (6.0 ± 0.3 log₁₀ CFU) of all infected animals (Fig. 1). Inactivation of *rel* (Δrel) or *relQ* ($\Delta relQ$) did not significantly alter *E. faecalis* colonization in bladders, but the level of recovery of $\Delta relQ$ bacteria from catheters was significantly lower (~ 0.8 -log₁₀ reduction; $P = 0.0027$ compared to OG1RF). On the other hand, the (p)ppGpp⁰ strain displayed ~ 0.8 -log₁₀ ($P = 0.0015$) and 1.5 -log₁₀ ($P < 0.0001$) reductions in CFU recovered from bladders and catheters, respectively (Fig. 1). The $\Delta codY$ strain phenocopied the (p)ppGpp⁰ strain, showing ~ 0.8 -log₁₀ reductions in CFU recovered from both bladders ($P = 0.0156$) and catheters ($P = 0.0031$) (Fig. 1). However, inactivation of *codY* in the (p)ppGpp⁰ background [(p)ppGpp⁰ $\Delta codY$ triple mutant] restored bacterial bladder and catheter colonization to near-parent-strain levels. Despite great variations from animal to animal but in relative agreement with the bacterial loads detected on catheters and in bladders, the OG1RF and Δrel strains were consistently able to ascend to the kidneys (Fig. 1C). However, the (p)ppGpp⁰ $\Delta codY$ triple mutant failed to consistently ascend to the kidneys, suggesting that the virulence of this strain may be partially compromised.

(p)ppGpp promotes timely growth of *E. faecalis* in human urine. The (p)ppGpp⁰ strain was previously shown to have growth and survival defects in whole blood and serum (15, 16). Interestingly, inactivation of *codY* in the (p)ppGpp⁰ background [(p)ppGpp⁰ $\Delta codY$] restored the (p)ppGpp⁰ growth defect in blood but not in serum (16). Here, we tested the ability of (p)ppGpp-defective [Δrel , $\Delta relQ$, and (p)ppGpp⁰] and *codY* [$\Delta codY$ and (p)ppGpp⁰ $\Delta codY$] strains to replicate in pooled human urine *ex vivo*. Despite the colonization defect in the murine CAUTI model (Fig. 1), the $\Delta codY$ strain grew as well as the parent and $\Delta relQ$ strains (Fig. 2). On the other hand, Δrel , (p)ppGpp⁰, and (p)ppGpp⁰ $\Delta codY$ strains grew slower in the first 12 h of incubation, with an ~ 0.6 -log₁₀ CFU difference at 3 and 7 h postinoculation (Fig. 2). Nevertheless, upon

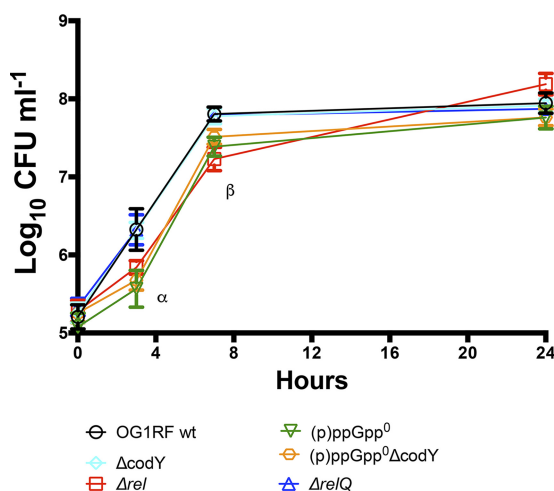


FIG 2 (p)ppGpp supports timely growth of *E. faecalis* in human urine. Growth of the parent *E. faecalis* strain OG1RF and its derivative mutant strains in pooled human urine was analyzed. Aliquots at selected time points were serially diluted and plated onto TSA plates for CFU enumeration. The graph shows the average log₁₀-transformed CFU (means and standard deviations) from three independent experiments. Mutant strains were compared to wild-type (wt) strain OG1RF by two-way ANOVA with Dunnett's multiple-comparison test. Asterisks indicate significant differences at 3 h of incubation for the Δrel , (p)ppGpp⁰, and (p)ppGpp⁰ $\Delta codY$ strains and at 7 h of incubation for the Δrel and (p)ppGpp⁰ $\Delta codY$ strains ($P < 0.0001$).

entering stationary phase, all strains reached similar growth yields and remained viable for at least 24 h.

(p)ppGpp and CodY support biofilm formation in urine. Biofilm formation on urinary catheters is critical for enterococcal CAUTI (22–24). This is exemplified by the observation that *E. faecalis* OG1RF requires the presence of a catheter to persist for more than 48 h in murine bladders (21). Follow-up studies revealed that catheterization, in mice and in humans, triggers an inflammatory response that releases the host protein fibrinogen, which is used by *E. faecalis* as a nutrient as well as a scaffold to adhere to and colonize the catheter surface (22–25). Taking into account that the reduction in bacterial counts of $\Delta relQ$, (p)ppGpp⁰, and $\Delta codY$ strains was more pronounced on catheters than in bladders (Fig. 1) and that (p)ppGpp supports long-term survival of *E. faecalis* in biofilms (12), we sought to investigate if the attenuated virulence of these strains in murine CAUTI was linked to a reduced ability to form biofilms on fibrinogen-coated surfaces in the presence of urine. Since catheterization normally elicits proteinuria in the host, and *E. faecalis* requires a protein source to optimally form biofilms in urine (22, 24), human urine was supplemented with bovine serum albumin (BSA). In agreement with the bacterial loads obtained from the implanted catheters (Fig. 1B), quantifications of *E. faecalis* biofilm biomass revealed that $\Delta relQ$, (p)ppGpp⁰, and $\Delta codY$ strains were deficient in biofilm production, while the Δrel strain phenocopied the parent OG1RF strain (Fig. 3A). Notably, inactivation of *codY* in the (p)ppGpp⁰ background alleviated the defective phenotype of the (p)ppGpp⁰ strain, albeit the differences between the (p)ppGpp⁰ $\Delta codY$ and OG1RF strains were still statistically significant.

As indicated above, the main factor involved in *E. faecalis* biofilm formation on urinary catheters is the production of the Ebp pilus, which binds directly to fibrinogen via the EbpA N-terminal domain (22, 26, 27). Quantification of EbpA via an enzyme-linked immunosorbent assay (ELISA) showed no noticeable reductions in EbpA production in any of the mutant strains (Fig. 3B), suggesting that the (p)ppGpp-CodY network promotes biofilm formation of fibrinogen-coated surfaces in an Ebp-independent manner.

Inactivation of *codY* restores the dysregulated metabolism of the (p)ppGpp⁰ strain. Previously, we proposed that the virulence attenuation of the (p)ppGpp⁰ strain

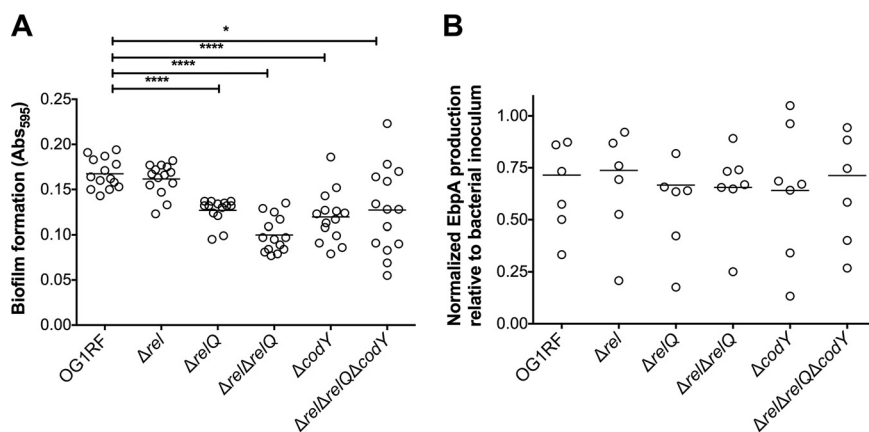


FIG 3 The (p)ppGpp-CodY network contributes to biofilm formation in urine. (A) Fibrinogen-coated 96-well polystyrene plates were incubated with *E. faecalis* strains for 48 h in human urine supplemented with 20 mg ml⁻¹ BSA. Plates were stained with 0.5% crystal violet, which was subsequently dissolved with 33% acetic acid, and the absorbance at 595 nm was measured. (B) EbpA quantification in urine. Strains were grown in urine plus BSA overnight prior to quantification of EbpA by an ELISA. EbpA surface exposure on *E. faecalis* cells was detected using mouse anti-EbpA^{Full} and HRP-conjugated goat anti-rabbit antisera, and the absorbance was determined at 450 nm. EbpA production titers were normalized against the bacterial titers. Experiments were performed independently in triplicate and analyzed by a two-tailed Mann-Whitney U test (*, $P < 0.05$; ****, $P < 0.0001$).

in different animal models is, in large part, due to the dysregulated metabolism caused by a lack of (p)ppGpp control (13, 14, 16). By monitoring H₂O₂ production and the culture pH, we provided the first evidence that inactivation of *codY* restored a balanced metabolism to the (p)ppGpp⁰ background strain (16). To obtain additional insights into the (p)ppGpp-CodY relationship, we used RNA sequencing (RNA-seq) technology to compare the transcriptomes of OG1RF, (p)ppGpp⁰, and (p)ppGpp⁰ Δ*codY* strains grown to mid-exponential phase in chemically defined FMC medium (28) supplemented with 10 mM glucose (FMCG medium). In the (p)ppGpp⁰ strain, 690 genes were differentially expressed compared to OG1RF ($P < 0.05$; 2-fold cutoff) (see Table S1 in the supplemental material), representing ~27% of the entire *E. faecalis* OG1RF genome. In agreement with a previous microarray analysis (14), multiple phosphotransferase systems (PTSs) as well as citrate, glycerol, malate, and serine utilization pathways were strongly induced in the (p)ppGpp⁰ strain under these conditions. A selected and representative number of dysregulated transport and metabolic genes in the (p)ppGpp⁰ strain are shown in Tables 1 and 2, respectively. The upregulation of alternate carbon metabolism genes that are expected to be under carbon catabolite repression (CCR) under the glucose-rich conditions of FMCG medium indicates that a complete lack of (p)ppGpp places *E. faecalis* in what we have originally termed a “transcriptionally relaxed” state (14). Compared to the parent strain, 737 genes (~29% of the entire genome) were differentially expressed in the (p)ppGpp⁰ Δ*codY* triple mutant strain ($P < 0.05$; 2-fold cutoff) (Table S2). Despite the even larger number of differentially expressed genes, inactivation of *codY* in the (p)ppGpp⁰ background strain normalized the transcription of 274 genes that were dysregulated in the (p)ppGpp⁰ background (Table S3). The great majority (~95%) of these genes were upregulated in the (p)ppGpp⁰ strain, supporting that deletion of *codY* abrogates, at least in part, the transcriptionally relaxed state of the (p)ppGpp⁰ mutant. More specifically, inactivation of *codY* in the (p)ppGpp⁰ background normalized the transcription (or brought it to levels much closer to that of the parent strain) of ~70 transport systems as well as over 130 metabolic genes, including citrate, glycerol, malate, and serine utilization pathways; dehydrogenases; and molybdenum-dependent enzymes (Table S3).

Dysregulation of c-di-AMP homeostasis may affect fitness of (p)ppGpp⁰ and Δ*codY* strains in urine. Previously, the Ebp pilus and two high-affinity manganese transporters, EfaCBA and MntH2, were shown to be essential for *E. faecalis* virulence in

TABLE 1 Transcriptional restoration of selected nutrient transport systems upon inactivation of *codY* in the (p)ppGpp⁰ background

Locus or gene name	Function(s)	Fold change ^a	
		(p)ppGpp ⁰	(p)ppGpp ⁰ $\Delta codY$
PTSs			
OG1RF_10341	PTS	+5.5	
OG1RF_10346	PTS	+4.8	
OG1RF_10433	PTS	+5.1	
OG1RF_10746	PTS	+8.2	
OG1RF_11236	PTS	+3.3	
OG1RF_11249	PTS	+3.1	-3.3
OG1RF_11512	PTS	+5.0	
OG1RF_11614	PTS	+4.2	
OG1RF_11780	PTS	+3.8	
OG1RF_12261	PTS	+4.6	
<i>bglP</i>	PTS, β -glucoside uptake	+7.4	
<i>frwB</i>	PTS, fructose uptake	+11.5	
<i>malX</i>	PTS, maltose uptake	+4.7	
<i>mltF2</i>	PTS, mannitol uptake	+7.1	
<i>scrA</i>	PTS, β -glucoside uptake	+3.4	
<i>sorA</i>	PTS, sorbose uptake	+32.5	
<i>treB</i>	PTS, trehalose uptake	+11.9	-2.0
<i>ulaB</i>	PTS, ascorbate uptake	+5.1	
ABC-type transporters			
OG1RF_10665	ABC-type transporter	+3.4	-2.5
OG1RF_10879	ABC-type transporter	+2.2	
OG1RF_11003	ABC-type transporter	+15.9	
OG1RF_11188	ABC-type transporter	+8.1	
OG1RF_11763	ABC-type transporter	+3.2	
OG1RF_11774	Sugar ABC-type transporter	+38.5	
OG1RF_12466	ABC-type transporter	+3.5	
<i>mdlB</i>	Multidrug ABC-type transporter	+3.2	
<i>modB</i>	Molybdenum transporter	+31.5	
T0	Oligopeptide transporter	-3.3	
<i>ziaA</i>	Zinc ABC-type transporter	+3.2	
Other porters			
OG1RF_11781	Sodium symporter	+5.3	
OG1RF_11873	Phosphate transporter	+4.5	-2.5
OG1RF_11954	Xanthine/uracil permease	+3.0	
OG1RF_12019	Gluconate symporter	+4.7	
OG1RF_12274	Major facilitator transporter	+21.3	
OG1RF_12280	Cytosine/purine permease	+5.4	
OG1RF_12572	Citrate transporter	+51.8	
<i>dctM</i>	Organic acid transporter	+4.5	
<i>glpF2</i>	Glycerol uptake	+11.0	

^aValues represent fold changes in transcription compared to the parent strain. All values shown were statistically significant ($P < 0.05$). Blank fields indicate that there were no significant differences between mutant and parent strains.

a mouse CAUTI model (27, 29). In an attempt to identify (p)ppGpp- and CodY-dependent processes directly relevant to enterococcal CAUTI, we compared the transcriptional profiles of these virulence factors in parent and mutant strains. In brief, quantitative real-time PCR (qPCR) was used to compare expression levels of selected genes in exponentially grown brain heart infusion (BHI) broth cultures of OG1RF, $\Delta codY$, (p)ppGpp⁰, and (p)ppGpp⁰ $\Delta codY$ strains before and after switching the cultures to pooled human urine. We found that the transcription of *ebpA* (coding for the pilin subunit), *efaC* (the ATP-binding subunit of the ABC-type transporter EfaCBA), and *mntH2* was strongly induced upon shifting the parent strain culture from BHI broth to urine (Fig. 4). While full upregulation of *efaC* in urine appears to be dependent on CodY, *ebpA* and *mntH2* transcription was differentially impacted by (p)ppGpp and CodY. Specifically, while inactivation of CodY ($\Delta codY$) limited the induction of these genes after transition to urine, the loss of (p)ppGpp induced the transcription of *ebpA* and

TABLE 2 Transcriptional profile of selected metabolic genes upon inactivation of *codY* in the (p)ppGpp⁰ background

Locus or gene name	Function	Fold change ^a	
		(p)ppGpp ⁰	(p)ppGpp ⁰ $\Delta codY$
Citrate metabolism			
OG1RF_10979	Citrate carrier	+31.2	
<i>citC</i>	Citrate metabolism	+17.0	-5.0
<i>citD</i>	Citrate metabolism	+18.7	-3.3
<i>citE</i>	Citrate metabolism	+15.6	-5.0
<i>citF</i>	Citrate metabolism	+15.0	-5.0
<i>citX</i>	Citrate metabolism	+13.4	-5.0
<i>citXG</i>	Citrate metabolism	+13.2	-2.0
Serine metabolism			
<i>sdaA</i>	Serine dehydratase	+103.5	
<i>sdaB</i>	Serine dehydratase	+94.5	-2.5
Glycerol metabolism			
<i>glpK</i>	Glycerol kinase	+5.7	-2.5
<i>glpO</i>	Glycerol-3-phosphate oxidase	+6.6	-2.5
<i>gldA2</i>	Glycerol dehydrogenase	+13.7	
Molybdenum metabolism			
OG1RF_11183	MOSC protein ^b	+30.1	
OG1RF_11185	Molybdopterin-binding protein	+25.6	
OG1RF_11944	Molybdenum hydroxylase	+29.7	
OG1RF_11951	Molybdenum hydroxylase	+10.8	-2.0
<i>moaA</i>	Molybdenum cofactor synthesis	+20.0	
<i>moaB</i>	Molybdenum cofactor synthesis	+27.1	
<i>moaC</i>	Molybdenum cofactor synthesis	+10.1	
<i>yedF2</i>	Selenium metabolism	+23.3	
<i>ygfJ</i>	Molybdenum hydroxylase	+20.6	
Other metabolic genes			
OG1RF_11942	Ferredoxin NADP ⁺ reductase	+23.4	
OG1RF_11943	Flavodoxin	+20.7	
<i>allD</i>	Ureidoglycolate dehydrogenase	+14.7	
<i>mdh</i>	Malate dehydrogenase	+16.5	
<i>fbp</i>	Fructose-1,6-bisphosphatase	+10.6	+3.9
<i>oadA</i>	Oxaloacetate decarboxylase	+14.2	-3.3
OG1RF_10107	Glycosyl hydrolase	+60.1	
<i>gcdB</i>	Glutaconyl-CoA decarboxylase	+15.0	-5.0
<i>arcC2</i>	Carbamate kinase	+17.4	
<i>gltA</i>	Glutamate synthase	+16.8	
OG1RF_11949	Cysteine desulfurase	+25.7	-2.5
<i>hydA</i>	Dihydropyrimidinase	+14.6	
OG1RF_11585	Ribosylpyrimidine nucleosidase	+11.1	-3.3
OG1RF_10108	Endoribonuclease	+48.7	
<i>endOF3</i>	<i>N</i> -Acetylglucosaminidase	+60.1	

^aValues represent fold changes in transcription compared to the parent strain. All values shown were statistically significant ($P < 0.05$). Blank fields indicate that there were no significant differences between mutant and parent strains.

^bMOSC, MOCO (molybdenum cofactor) sulfurase C-terminal.

mntH2 by ~10-fold. The simultaneous inactivation of *codY* in the (p)ppGpp⁰ background [(p)ppGpp⁰ $\Delta codY$] modestly raised *ebpA* but fully restored *mntH2* mRNA levels (Fig. 4).

We also assessed transcription levels of genes coding for enzymes involved in the metabolism of *c*-di-AMP, a nucleotide second messenger essential for osmotic stress survival and whose regulatory network appears to be intertwined with the (p)ppGpp regulatory network in other bacteria (30–34). In the OG1RF strain, transcription of the *c*-di-AMP cyclase *cdaA* was not significantly altered upon transition from BHI broth to urine; however, transcription of both *c*-di-AMP hydrolases (*pde* and *gdpP*) was induced by ~50- and 100-fold, respectively (Fig. 4). While induction of *gdpP* was dependent on CodY, activation of *pde* in urine was not as robust in all mutant strains. Unexpectedly,

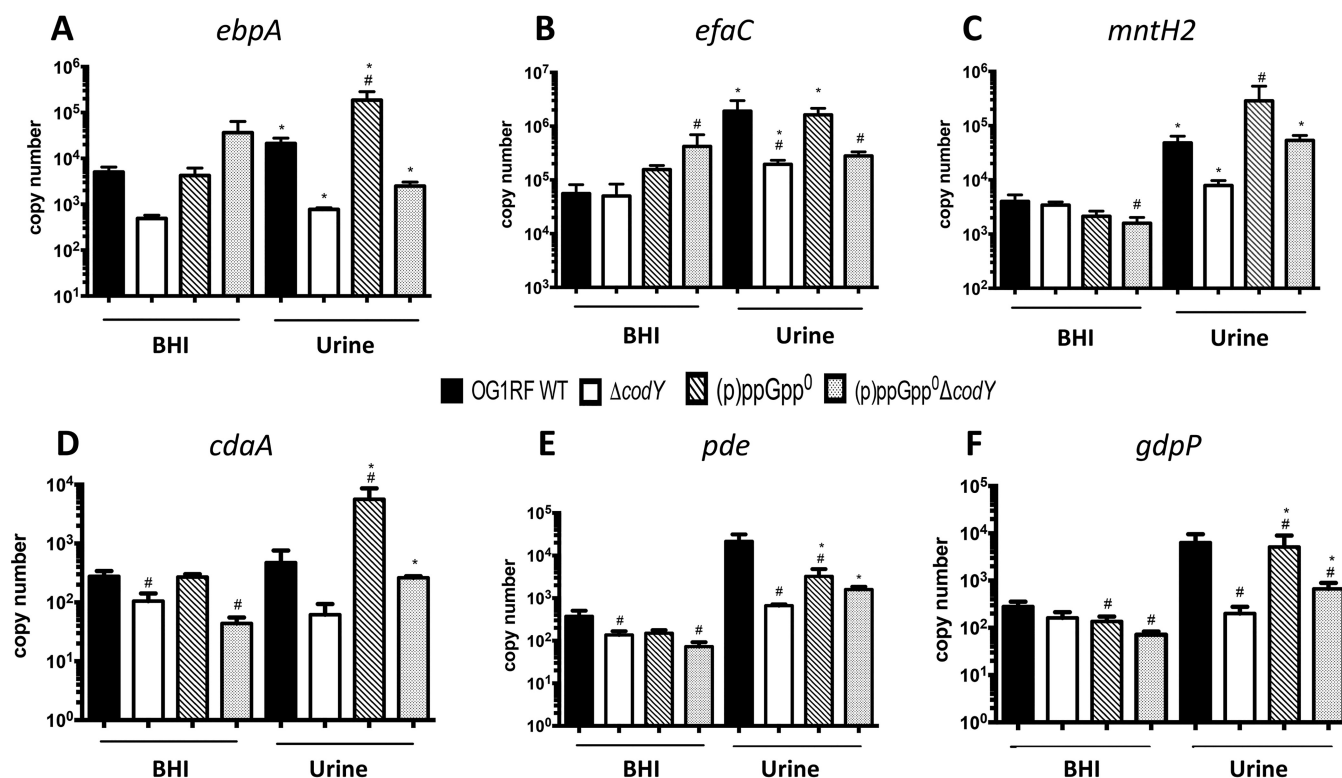


FIG 4 Transcript levels of selected genes in OG1RF, (p)ppGpp⁰, $\Delta codY$, and (p)ppGpp⁰ $\Delta codY$ cultures in BHI broth or human urine. The *E. faecalis* OG1RF wild-type (WT), (p)ppGpp⁰, (p)ppGpp⁰ $\Delta codY$, and $\Delta codY$ strains were grown in BHI broth to the mid-exponential growth phase. Cell pellets were washed thoroughly and then exposed to pooled human urine and fresh BHI broth for 30 min. The transcript levels of *ebpA* (A), *efaC* (B), *mntH2* (C), *cdaA* (D), *pde* (E), and *gdpP* (F) were determined by quantitative real-time PCR. The bar graphs show averages and standard deviations of results from three independent experiments performed in triplicate. Differences seen with the same strains under different conditions (#) or between parent and mutant strains under the same growth conditions (*) were compared via Student's *t* test or ANOVA with a multiple-comparison test, respectively ($P < 0.05$).

cdaA transcription was strongly induced (~50-fold) in the (p)ppGpp⁰ strain when shifted from BHI broth to urine, suggesting that c-di-AMP levels may be dysregulated in the (p)ppGpp⁰ strain during CAUTI. Notably, pools of c-di-AMP must be tightly controlled given that it is essential for growth but also highly toxic when present at high concentrations (35).

DISCUSSION

In this report, we show that basal (p)ppGpp pools and the transcriptional regulator CodY mediate the virulence of *E. faecalis* in a murine CAUTI model. These results corroborate previous findings that changes in basal levels of (p)ppGpp contribute to the virulence of *E. faecalis* (10, 11, 13, 15, 17) and show, for the first time, that CodY regulation is also important for the virulence of *E. faecalis*. Despite the attenuated virulence of the $\Delta codY$, $\Delta relQ$, and (p)ppGpp⁰ strains, simultaneous inactivation of both regulatory pathways [(p)ppGpp⁰ $\Delta codY$ strain] restored virulence to near-parent-strain levels. While this finding may appear contradictory, it is in line with previous studies showing that inactivation of *codY* restores the virulence of (p)ppGpp⁰ strains of *Listeria monocytogenes* and *Staphylococcus aureus* (36, 37).

Despite the significance of the (p)ppGpp-CodY regulatory network in enterococcal CAUTI, the differences in total bacteria recovered from the infected organs observed here were not as robust as those observed in a previous investigation that depicted the essential role of the manganese transporters EfaCBA and MntH2 in CAUTI (29). Interestingly, we have shown that several phenotypes of the (p)ppGpp⁰ strain can be reverted by manganese supplementation, which is used to help the cells cope with high levels of endogenously produced reactive oxygen species (ROS) (16). Thus, it is conceivable that the attenuated virulence of the (p)ppGpp⁰ strain shown here can

be traced to manganese homeostasis and thereby restored in mice fed a high-manganese diet or in animals that are unable to sequester manganese during infection (calprotectin-defective mice).

The association between (p)ppGpp and CodY, by which (p)ppGpp upregulates gene transcription via GTP depletion and the concomitant alleviation of CodY repression, has been well established (20). We previously found that the (p)ppGpp and CodY regulatory networks are also intertwined in *E. faecalis* by showing that inactivation of *codY* restored phenotypes of the (p)ppGpp⁰ strain, such as the inability to grow in whole blood *ex vivo* and reduced virulence in the *G. mellonella* invertebrate model (16). By comparing final culture pH and H₂O₂ production of (p)ppGpp⁰ and (p)ppGpp⁰ Δ *codY* strains, we hypothesized that deletion of *codY* restores a balanced metabolism to the (p)ppGpp⁰ strain (14, 16). The RNA-seq analysis reported here clearly supports this observation, as multiple genes coding for alternate carbon utilization pathways were strongly upregulated in the (p)ppGpp⁰ strain but not in the (p)ppGpp⁰ Δ *codY* triple mutant strain.

Our results also indicate that restoration of global metabolism in the (p)ppGpp⁰ Δ *codY* strain compared to the (p)ppGpp⁰ strain may be particularly relevant in experimental CAUTI. Specifically, we show that while the absence of either (p)ppGpp or CodY results in defects in biofilm formation *in vitro* and *in vivo*, simultaneous inactivation of the (p)ppGpp and CodY regulatory systems restores CAUTI virulence and partially restores *in vitro* biofilm formation to near-parent-strain levels (Fig. 1 and 3). Considering that the levels of the surface protein EbpA were not altered in any of the mutant strains (Fig. 3), we propose that (p)ppGpp and CodY promote biofilm formation on urinary catheters by mediating the metabolic rearrangements required for biofilm growth and survival in urine. In fact, a comparative transcriptome analysis reveals that several metabolic pathways previously identified as being relevant to enterococcal adaptation to growth in urine (38) overlap the (p)ppGpp and CodY regulons (13, 14, 20). For example, transcriptional activation of alternate carbon utilization and amino acid biosynthesis/transport genes in response to the relatively low urinary concentrations of amino acids and glucose (38–41) is shown here to be regulated by (p)ppGpp and CodY (Tables 1 and 2; see also Table S1 in the supplemental material) (13, 14, 20).

In an attempt to identify specific (p)ppGpp- and CodY-regulated processes that are important for CAUTI, we used qPCR to compare transcription levels of known virulence factors, such as the Ebp pilus and the metal transporters EfaCBA and MntH2 (27, 29), in parent and mutant strains. Although there were significant alterations in the transcription of *ebpA*, *efaC*, and *mntH2* in the (p)ppGpp and *codY* mutant strains, it was not possible to establish a firm correlation between the transcriptional expression of these virulence factors and the attenuated virulence phenotypes shown in Fig. 1. Due to the association of c-di-AMP signaling with biofilm formation (33, 34) and adaptation to osmotic stress (31, 32), two relevant traits during CAUTI, and the previous linkage with (p)ppGpp signaling (30, 35, 42), we similarly assessed gene expression of the enzymes responsible for c-di-AMP synthesis (*cdaA*) and degradation (*pde* and *gdpP*). c-di-AMP is an emerging regulatory nucleotide shown to control a number of cellular processes, including potassium homeostasis, osmotic adaptation, and biofilm formation (35). In addition, previous investigations revealed an intricate but poorly understood association between the c-di-AMP and (p)ppGpp signaling networks, in which (p)ppGpp regulates c-di-AMP levels by serving as an allosteric regulator of c-di-AMP phosphodiesterase (PDE) enzymes, while c-di-AMP stimulates (p)ppGpp synthesis via an unknown mechanism (30, 35, 42). The strong activation of *pde* and *gdpP* in the parent strain upon a shift to urine suggests that intracellular c-di-AMP levels decrease in the presence of urine. This is not surprising considering that salt concentrations in urine are generally high (average osmolarity of between 300 and 900 mosM/kg H₂O) and that low c-di-AMP levels are associated with bacterial salt tolerance (43), whereas increased c-di-AMP levels are linked to salt hypersensitivity (44–46). Interestingly, the level of transcription of the c-di-AMP synthetase gene (*cdaA*) in urine was approximately

100-fold higher in the (p)ppGpp⁰ strain than in the parent strain, indicating that c-di-AMP homeostasis may be severely disrupted in the (p)ppGpp⁰ strain. Finally, transcription of the *pde* and *gdpP* genes was not as strongly induced (or not induced at all) in the (p)ppGpp⁰ and $\Delta codY$ strains. While the cellular levels of c-di-AMP in cells grown in urine remain to be determined, and the possibility of (p)ppGpp/c-di-AMP signaling cross talk in *E. faecalis* remains to be confirmed, the qPCR analysis suggests that *E. faecalis* decreases c-di-AMP pools to adjust its metabolism to the environment (i.e., high osmolality) encountered in urine.

By comparing the genes restored by *codY* inactivation in our RNA-seq analysis (Tables 1 and 2 and Table S1) to the transcriptome of *E. faecalis* OG1RF grown in urine (38), several other common pathways were identified, providing additional leads as to why alleviation of CodY repression restored the biofilm defect of the (p)ppGpp⁰ strain. Specifically, Vebø et al. showed that transcription of a major glycerol uptake system was induced when the OG1RF strain was grown in urine *ex vivo*, suggesting that *E. faecalis* utilizes glycerol as a source of energy to grow and survive in urine (38). Notably, aerobic metabolism of glycerol by the GlpO enzyme is also the main source of H₂O₂ generation in *E. faecalis* (47), and *E. faecalis* activates the transcription of several oxidative genes (such as *sodA*, *npr*, and *trxB*) when grown in urine (38), possibly to cope with increased ROS generation caused by aerobic glycerol metabolism. In agreement with previous microarray data (14), the current RNA-seq analysis revealed that transcription of glycerol catabolic genes, such as *glpO* and *gldA2*, was activated by 6-fold or more in the (p)ppGpp⁰ strain (Table 2 and Table S1), likely augmenting ROS production in the urinary tract. Another possibility, which is not mutually exclusive from the others, is that the strong (~20-fold) upregulation of molybdenum metabolism genes in the (p)ppGpp⁰ strain is disadvantageous to *E. faecalis* when grown in the urinary tract environment. Molybdenum is a rare transition metal that functions as a cofactor of several redox-active enzymes (48–50); it should be noted that urothione, the degradation product of the molybdenum cofactor in humans, is excreted in urine (51). In contrast to other metal cofactors, molybdenum is catalytically active only when complexed with a pterin-based scaffold, forming the Moco prosthetic group (50). The Moco biosynthetic genes that are highly induced in the (p)ppGpp⁰ mutant strain code for enzymes that require GTP and the oxygen-reactive iron and copper metals (50), possibly linking molybdenum metabolism to (p)ppGpp and oxidative stress. Finally, *E. faecalis* appears to downregulate serine catabolism in urine (38). However, serine dehydratases were among the most highly expressed genes in the (p)ppGpp⁰ strain (~100-fold), likely favoring pyruvate generation instead of protein synthesis. While it is unknown how serine catabolism and dysregulation of other metabolic and transport pathways affect biofilm formation and virulence in *E. faecalis*, alleviation of CodY repression for the most part restored the transcription of these genes to wild-type levels.

Collectively, the results presented here reveal that (p)ppGpp and CodY support the presence of *E. faecalis* in the catheterized murine urinary tract by controlling the metabolic arrangements necessary for the fitness of *E. faecalis* in this environment and, possibly, by modulating biofilm formation. Future studies using global transcriptome and metabolome analyses of (p)ppGpp-deficient and CodY-deficient strains recovered directly from CAUTI, coupled with characterization of pathways relevant to biofilm formation in urine, are necessary to fully understand how alleviation of CodY repression restores biofilm formation in the absence of (p)ppGpp. In addition, the relevance of c-di-AMP signaling to enterococcal CAUTI and the relationship between (p)ppGpp and c-di-AMP signaling pathways will warrant further investigations. In this regard, work is under way to determine the scope and targets of c-di-AMP regulation in *E. faecalis*. These studies should expand our mechanistic understanding of how global metabolic regulators such as CodY, (p)ppGpp, and possibly c-di-AMP mediate enterococcal pathogenesis in the urinary tract and beyond.

MATERIALS AND METHODS

Bacterial strains and growth conditions. The parent *E. faecalis* OG1RF strain and its derivative Δrel , $\Delta relQ$, $\Delta rel \Delta relQ$ [(p)ppGpp⁰], $\Delta codY$, and (p)ppGpp⁰ $\Delta codY$ strains were previously described (10, 16). All strains were routinely grown in BHI broth at 37°C. For RNA sequencing (RNA-seq) analysis, cultures of *E. faecalis* OG1RF, (p)ppGpp⁰, and (p)ppGpp⁰ $\Delta codY$ strains grown overnight were diluted in a 1:100 ratio in 50 ml of chemically defined FMC medium (28) supplemented with 10 mM glucose (FMCG medium) and allowed to grow statically at 37°C to an optical density at 600 nm (OD₆₀₀) of 0.3. Growth in pooled human urine from healthy donors (Lee Biosolutions) was monitored as described previously, with minor modifications (29). Briefly, cultures grown overnight were diluted 1:100 in phosphate-buffered saline (PBS) and inoculated at a 1:100 dilution for growth assessment in urine. Cultures were incubated aerobically at 37°C, and at selected time points, aliquots were serially diluted and plated onto tryptic soy agar (TSA) plates for CFU determination. To determine the transcriptional responses of selected genes upon transition from laboratory medium to human urine, cultures grown overnight in BHI broth were diluted 1:20 in 5 ml of fresh sterile BHI broth and allowed to grow statically at 37°C to an OD₆₀₀ of 0.5. The bacterial cells were washed twice with PBS (pH 7.0) and pelleted down by centrifugation at 2,500 rpm for 8 min. After washing, pellets were resuspended in 7.5 ml filter-sterilized urine and incubated at 37°C for 30 min. The controls were resuspended in the same volume of fresh BHI broth and incubated at 37°C for 30 min.

Mouse catheter implantation and infection. The mice used in this study were 6-week-old female wild-type C57BL/6Ncr mice purchased from Charles River Laboratories. Mice were subjected to transurethral implantation and inoculated as previously described (21). Mice were anesthetized by inhalation of isoflurane and implanted with a 5-mm-long platinum-cured silicone catheter. When indicated, mice were infected immediately following catheter implantation with 50 μ l of $\sim 2 \times 10^7$ CFU of bacteria in PBS introduced into the bladder lumen by transurethral inoculation as previously described (21). To harvest the catheters and organs, mice were sacrificed at 3 days postinfection by cervical dislocation after anesthesia inhalation; the silicone catheter, bladder, and kidneys were aseptically harvested. The Washington University Animal Studies Committee approved all mouse infections and procedures as part of protocol number 20150226. All animal care was consistent with the *Guide for the Care and Use of Laboratory Animals* from the National Research Council (52).

Biofilm formation in human urine. For assessment of biofilm formation on fibrinogen-coated 96-well polystyrene plates (Grenier CellStar), wells were coated overnight at 4°C with 100 μ g ml⁻¹ human fibrinogen free of plasminogen and von Willebrand factor (Enzyme Research Laboratory). The next day, *E. faecalis* cultures grown overnight were diluted to an OD₆₀₀ of 0.2 in BHI broth. The diluted cultures were centrifuged, washed three times with 1 \times PBS, and diluted 1:100 in urine supplemented with 20 mg ml⁻¹ BSA. Bacterial cells were allowed to attach to the fibrinogen-coated plate at 37°C under static conditions as described previously (29, 53). After 24 h, microplates were washed with PBS to remove unbound bacteria, and biofilm formation was assessed by staining wells with crystal violet as previously described (53). Excess dye was removed by rinsing with sterile water, and the plates were then allowed to dry at room temperature. Biofilms were resuspended with 200 μ l of 33% acetic acid, and the absorbance at 595 nm was measured on a microplate reader (Molecular Devices). Experiments were performed independently in triplicate per condition and per experiment.

Presence of EbpA on the cell surface of (p)ppGpp- and CodY-deficient strains. Surface expression of EbpA by *E. faecalis* OG1RF and derivatives was determined by an ELISA as previously described (23). Bacterial strains were grown for 18 h in urine supplemented with 20 mg ml⁻¹ of BSA. Next, bacterial cells were washed (3 times) with PBS, normalized to an OD₆₀₀ of 0.5, resuspended with 50 mM carbonate buffer (pH 9.6) containing 0.1% sodium azide, and used (100 μ l) to coat Immulon 4HBX microtiter plates overnight at 4°C. The next day, plates were washed 3 times with PBS containing 0.05% Tween 20 (PBS-T) to remove unbound bacteria and blocked for 2 h with 1.5% BSA–0.1% sodium azide–PBS, followed by three washes with PBS-T. EbpA surface expression was detected using mouse anti-EbpA^{F^{ull}} antiserum, which was diluted 1:100 in dilution buffer (PBS with 0.05% Tween 20, 0.1% BSA, and 0.5% methyl- α -D-mannopyranoside) before serial dilutions were performed. A 100- μ l volume was added to the plate, and the reaction mixture was incubated for 2 h. Subsequently, plates were washed with PBS-T, incubated for 1 h with horseradish peroxidase (HRP)-conjugated goat anti-rabbit antiserum (1:2,000), and washed again with PBS-T. Detection was performed using a TMB (3,3',5,5'-tetramethylbenzidine) substrate reagent set (BD). The reaction mixtures were incubated for 5 min to allow color to develop, and the reactions were then stopped by the addition of 1.0 M sulfuric acid. The absorbance was determined at 450 nm. Titers were defined by the last dilution with an A₄₅₀ of at least 0.2. As an additional control, rabbit anti-*Streptococcus* group D antiserum was used to verify that whole cells of all strains were bound to the microtiter plates at similar levels. EbpA expression titers were normalized against the bacterial titers at the same dilution.

RNA-seq analysis. Cells grown in FMCG medium to an OD₆₀₀ of 0.3 were collected by centrifugation at 4,000 rpm for 20 min at 4°C and resuspended in 4 ml of a sterile RNA-stabilizing solution [3.5 M (NH₄)₂SO₄, 16.6 mM sodium citrate, and 13.3 mM EDTA, adjusted to a pH of 5.2 with H₂SO₄]. After a 10-min incubation at room temperature, cells were centrifuged at 4,000 rpm for 30 min at 4°C, and pellets were stored at -80°C. RNA was extracted using the hot acid-phenol-chloroform method as previously described (54). Subsequently, precipitated RNA was treated once with DNase I (Ambion, Carlsbad, CA), followed by a second DNase I treatment using the DNA-free kit (Ambion) to completely remove DNA, divalent cations, and traces of the DNase I enzyme. RNA concentrations were quantified with the NanoDrop 1000 spectrophotometer (NanoDrop, Wilmington, DE), and RNA quality was assessed with the Agilent bioanalyzer (Agilent, Santa Clara, CA). RNA-seq, data processing, and statistical analysis were

performed at the University of Rochester Genomics Research Center (UR-GRC) using the Illumina platform as previously described (55).

Real-time quantitative PCR analysis. Cultures were pelleted at 2,500 rpm for 8 min at 4°C. The bacterial pellets were resuspended in 1 ml of RNA protect and incubated for 5 min at room temperature, followed by centrifugation at 2,500 rpm for 8 min at 4°C. At that point, the bacterial pellets were kept at –80°C until ready for RNA extraction. Cells were resuspended in TE buffer (10 mM Tris Cl [pH 8], 1 mM EDTA) and 10% SDS and homogenized for three 30-s cycles, with 2 min on ice between cycles. The nucleic acids were retrieved from the total protein by phenol-chloroform (5:1) extraction. The inorganic phase was resuspended in 0.7 ml RLT buffer (Qiagen) supplemented with 1% β -mercaptoethanol, and RNA was purified using an RNeasy minikit (Qiagen), including the on-column DNase treatment recommended by the supplier. To further reduce DNA contamination, RNA samples were treated with DNase I (Ambion) at 37°C for 30 min and repurified using the RNeasy minikit (Qiagen). RNA concentrations were determined using the NanoDrop spectrophotometer. Reverse transcription and real-time PCR were carried out according to protocols described previously (54), using the primer sets indicated in Table S4 in the supplemental material.

Statistical analysis. Data sets were analyzed using GraphPad Prism 6.0 software unless otherwise noted. \log_{10} -transformed CFU values from urine growth curves were analyzed via two-way analysis of variance (ANOVA) followed by a comparison posttest. For CAUTI experiments, biofilm assays, and EbpA ELISAs, a two-tailed Mann-Whitney U test was performed. RNA-seq processing and the subsequent statistical analysis were performed at UR-GRC as previously described (55). qPCR data were analyzed by Student's *t* test and ANOVA with a multiple-comparison test.

Data availability. Gene expression data have been deposited in the NCBI Gene Expression Omnibus (GEO) database under GEO series accession number [GSE131749](https://www.ncbi.nlm.nih.gov/geo/query/acc.cgi?acc=GSE131749).

SUPPLEMENTAL MATERIAL

Supplemental material for this article may be found at <https://doi.org/10.1128/mSphere.00392-19>.

TABLE S1, XLSX file, 0.1 MB.

TABLE S2, XLSX file, 0.1 MB.

TABLE S3, XLSX file, 0.1 MB.

TABLE S4, DOCX file, 0.01 MB.

ACKNOWLEDGMENTS

This research was supported by National Institute of Allergy and Infectious Diseases grants AI135158 (J.A.L.) and AI10874901 (S.J.H.) and National Institute of Diabetes and Digestive and Kidney Diseases grants DK051406 (S.J.H.) and P50-DK0645400 (S.J.H.). C.C.-W. was supported by American Heart Association GSA predoctoral fellowship 16PRE29860000. The funders had no role in study design, data collection and analysis, decision to publish, or preparation of the manuscript.

REFERENCES

1. Reed D, Kemmerly SA. 2009. Infection control and prevention: a review of hospital-acquired infections and the economic implications. *Ochsner J* 9:27–31.
2. Foxman B. 2010. The epidemiology of urinary tract infection. *Nat Rev Urol* 7:653–660. <https://doi.org/10.1038/nrurol.2010.190>.
3. Lobdell KW, Stamou S, Sanchez JA. 2012. Hospital-acquired infections. *Surg Clin North Am* 92:65–77. <https://doi.org/10.1016/j.suc.2011.11.003>.
4. Flores-Mireles AL, Walker JN, Caparon M, Hultgren SJ. 2015. Urinary tract infections: epidemiology, mechanisms of infection and treatment options. *Nat Rev Microbiol* 13:269–284. <https://doi.org/10.1038/nrmicro3432>.
5. Lleo M, Bonato B, Tafi MC, Caburlo G, Benedetti D, Canepari P. 2007. Adhesion to medical device materials and biofilm formation capability of some species of enterococci in different physiological states. *FEMS Microbiol Lett* 274:232–237. <https://doi.org/10.1111/j.1574-6968.2007.00836.x>.
6. Niveditha S, Pramodhini S, Umadevi S, Kumar S, Stephen S. 2012. The isolation and the biofilm formation of uropathogens in the patients with catheter associated urinary tract infections (UTIs). *J Clin Diagn Res* 6:1478–1482. <https://doi.org/10.7860/JCDR/2012/4367.2537>.
7. Arias CA, Murray BE. 2012. The rise of the *Enterococcus*: beyond vancomycin resistance. *Nat Rev Microbiol* 10:266–278. <https://doi.org/10.1038/nrmicro2761>.
8. Potrykus K, Cashel M. 2008. (p)ppGpp: still magical? *Annu Rev Microbiol* 62:35–51. <https://doi.org/10.1146/annurev.micro.62.081307.162903>.
9. Dalebroux ZD, Svensson SL, Gaynor EC, Swanson MS. 2010. ppGpp conjures bacterial virulence. *Microbiol Mol Biol Rev* 74:171–199. <https://doi.org/10.1128/MMBR.00046-09>.
10. Abranches J, Martinez AR, Kajfasz JK, Chavez V, Garsin DA, Lemos JA. 2009. The molecular alarmone (p)ppGpp mediates stress responses, vancomycin tolerance, and virulence in *Enterococcus faecalis*. *J Bacteriol* 191:2248–2256. <https://doi.org/10.1128/JB.01726-08>.
11. Yan X, Zhao C, Budin-Verneuil A, Hartke A, Rince A, Gilmore MS, Auffray Y, Pichereau V. 2009. The (p)ppGpp synthetase RelA contributes to stress adaptation and virulence in *Enterococcus faecalis* V583. *Microbiology* 155:3226–3237. <https://doi.org/10.1099/mic.0.026146-0>.
12. Chávez de Paz LE, Lemos JA, Wickström C, Sedgley CM. 2012. Role of (p)ppGpp in biofilm formation by *Enterococcus faecalis*. *Appl Environ Microbiol* 78:1627–1630. <https://doi.org/10.1128/AEM.07036-11>.
13. Gaca AO, Abranches J, Kajfasz JK, Lemos JA. 2012. Global transcriptional analysis of the stringent response in *Enterococcus faecalis*. *Microbiology* 158:1994–2004. <https://doi.org/10.1099/mic.0.060236-0>.
14. Gaca AO, Kajfasz JK, Miller JH, Liu K, Wang JD, Abranches J, Lemos JA. 2013. Basal levels of (p)ppGpp in *Enterococcus faecalis*: the magic beyond the stringent response. *mBio* 4:e00646-13. <https://doi.org/10.1128/mBio.00646-13>.
15. Frank KL, Colomer-Winter C, Grindle SM, Lemos JA, Schlievert PM, Dunny GM. 2014. Transcriptome analysis of *Enterococcus faecalis* during mammalian infection shows cells undergo adaptation and exist in a stringent response state. *PLoS One* 9:e115839. <https://doi.org/10.1371/journal.pone.0115839>.

16. Colomer-Winter C, Gaca AO, Lemos JA. 2017. Association of metal homeostasis and (p)ppGpp regulation in the pathophysiology of *Enterococcus faecalis*. *Infect Immun* 85:e00260-17. <https://doi.org/10.1128/IAI.00260-17>.
17. Colomer-Winter C, Gaca AO, Chuang-Smith ON, Lemos JA, Frank KL. 2018. Basal levels of (p)ppGpp differentially affect the pathogenesis of infective endocarditis in *Enterococcus faecalis*. *Microbiology* 164: 1254–1265. <https://doi.org/10.1099/mic.0.000703>.
18. Gaca AO, Colomer-Winter C, Lemos JA. 2015. Many means to a common end: the intricacies of (p)ppGpp metabolism and its control of bacterial homeostasis. *J Bacteriol* 197:1146–1156. <https://doi.org/10.1128/JB.02577-14>.
19. Gaca AO, Kudrin P, Colomer-Winter C, Beljantseva J, Liu K, Anderson B, Wang JD, Rejman D, Potrykus K, Cashel M, Hauryluk V, Lemos JA. 2015. From (p)ppGpp to (pp)pGpp: characterization of regulatory effects of pGpp synthesized by the small alarmone synthetase of *Enterococcus faecalis*. *J Bacteriol* 197:2908–2919. <https://doi.org/10.1128/JB.00324-15>.
20. Geiger T, Wolz C. 2014. Intersection of the stringent response and the CodY regulon in low GC Gram-positive bacteria. *Int J Med Microbiol* 304:150–155. <https://doi.org/10.1016/j.ijmm.2013.11.013>.
21. Guiton PS, Hung CS, Hancock LE, Caparon MG, Hultgren SJ. 2010. Enterococcal biofilm formation and virulence in an optimized murine model of foreign body-associated urinary tract infections. *Infect Immun* 78:4166–4175. <https://doi.org/10.1128/IAI.00711-10>.
22. Flores-Mireles AL, Pinkner JS, Caparon MG, Hultgren SJ. 2014. EbpA vaccine antibodies block binding of *Enterococcus faecalis* to fibrinogen to prevent catheter-associated bladder infection in mice. *Sci Transl Med* 6:254ra127. <https://doi.org/10.1126/scitranslmed.3009384>.
23. Flores-Mireles AL, Walker JN, Potretzke A, Schreiber HL, IV, Pinkner JS, Bauman TM, Park AM, Desai A, Hultgren SJ, Caparon MG. 2016. Antibody-based therapy for enterococcal catheter-associated urinary tract infections. *mBio* 7:e01653-16. <https://doi.org/10.1128/mBio.01653-16>.
24. Xu W, Flores-Mireles AL, Cusumano ZT, Takagi E, Hultgren SJ, Caparon MG. 2017. Host and bacterial proteases influence biofilm formation and virulence in a murine model of enterococcal catheter-associated urinary tract infection. *NPJ Biofilms Microbiomes* 3:28. <https://doi.org/10.1038/s41522-017-0036-z>.
25. Flores-Mireles AL, Walker JN, Bauman TM, Potretzke AM, Schreiber HL, IV, Park AM, Pinkner JS, Caparon MG, Hultgren SJ, Desai A. 2016. Fibrinogen release and deposition on urinary catheters placed during urological procedures. *J Urol* 196:416–421. <https://doi.org/10.1016/j.juro.2016.01.100>.
26. Nallapareddy SR, Singh KV, Sillanpaa J, Zhao M, Murray BE. 2011. Relative contributions of Ebp pili and the collagen adhesin ace to host extracellular matrix protein adherence and experimental urinary tract infection by *Enterococcus faecalis* OG1RF. *Infect Immun* 79:2901–2910. <https://doi.org/10.1128/IAI.00038-11>.
27. Nielsen HV, Guiton PS, Kline KA, Port GC, Pinkner JS, Neiers F, Normark S, Henriques-Normark B, Caparon MG, Hultgren SJ. 2012. The metal ion-dependent adhesion site motif of the *Enterococcus faecalis* EbpA pilin mediates pilus function in catheter-associated urinary tract infection. *mBio* 3:e00177-12. <https://doi.org/10.1128/mBio.00177-12>.
28. Terleckyj B, Willett NP, Shockman GD. 1975. Growth of several cariogenic strains of oral streptococci in a chemically defined medium. *Infect Immun* 11:649–655.
29. Colomer-Winter C, Flores-Mireles AL, Baker SP, Frank KL, Lynch AJL, Hultgren SJ, Kitten T, Lemos JA. 2018. Manganese acquisition is essential for virulence of *Enterococcus faecalis*. *PLoS Pathog* 14:e1007102. <https://doi.org/10.1371/journal.ppat.1007102>.
30. Whiteley AT, Pollock AJ, Portnoy DA. 2015. The PAMP c-di-AMP is essential for *Listeria monocytogenes* growth in rich but not minimal media due to a toxic increase in (p)ppGpp. *Cell Host Microbe* 17: 788–798. <https://doi.org/10.1016/j.chom.2015.05.006>.
31. Whiteley AT, Garelis NE, Peterson BN, Choi PH, Tong L, Woodward JJ, Portnoy DA. 2017. c-di-AMP modulates *Listeria monocytogenes* central metabolism to regulate growth, antibiotic resistance and osmoregulation. *Mol Microbiol* 104:212–233. <https://doi.org/10.1111/mmi.13622>.
32. Pham HT, Nhiep NTH, Vu TNM, Huynh TN, Zhu Y, Huynh ALD, Chakraborti A, Marcellin E, Lo R, Howard CB, Bansal N, Woodward JJ, Liang ZX, Turner MS. 2018. Enhanced uptake of potassium or glycine betaine or export of cyclic-di-AMP restores osmoresistance in a high cyclic-di-AMP *Lactococcus lactis* mutant. *PLoS Genet* 14:e1007574. <https://doi.org/10.1371/journal.pgen.1007574>.
33. Townsley L, Yannarell SM, Huynh TN, Woodward JJ, Shank EA. 2018. Cyclic di-AMP acts as an extracellular signal that impacts *Bacillus subtilis* biofilm formation and plant attachment. *mBio* 9:e00341-18. <https://doi.org/10.1128/mBio.00341-18>.
34. Teh WK, Dramsi S, Tolker-Nielsen T, Yang L, Givskov M. 2019. Increased intracellular cyclic di-AMP levels sensitize *Streptococcus gallolyticus* subsp. *gallolyticus* to osmotic stress and reduce biofilm formation and adherence on intestinal cells. *J Bacteriol* 201:e00597-18. <https://doi.org/10.1128/JB.00597-18>.
35. Commichau FM, Heidemann JL, Ficner R, Stulke J. 2019. Making and breaking of an essential poison: the cyclases and phosphodiesterases that produce and degrade the essential second messenger cyclic di-AMP in bacteria. *J Bacteriol* 201:e00462-18. <https://doi.org/10.1128/JB.00462-18>.
36. Bennett HJ, Pearce DM, Glenn S, Taylor CM, Kuhn M, Sonenshein AL, Andrew PW, Roberts IS. 2007. Characterization of *relA* and *codY* mutants of *Listeria monocytogenes*: identification of the CodY regulon and its role in virulence. *Mol Microbiol* 63:1453–1467. <https://doi.org/10.1111/j.1365-2958.2007.05597.x>.
37. Geiger T, Goerke C, Fritz M, Schafer T, Ohlsen K, Liebecke M, Lalk M, Wolz C. 2010. Role of the (p)ppGpp synthase RSH, a RelA/SpoT homolog, in stringent response and virulence of *Staphylococcus aureus*. *Infect Immun* 78:1873–1883. <https://doi.org/10.1128/IAI.01439-09>.
38. Vebo HC, Solheim M, Snipen L, Nes IF, Brede DA. 2010. Comparative genomic analysis of pathogenic and probiotic *Enterococcus faecalis* isolates, and their transcriptional responses to growth in human urine. *PLoS One* 5:e12489. <https://doi.org/10.1371/journal.pone.0012489>.
39. Kirchmann H, Pettersson S. 1995. Human urine—chemical composition and fertilizer use efficiency. *Fertilizer Res* 40:149–154. <https://doi.org/10.1007/BF00750100>.
40. Shaykhtudinov RA, MacInnis GD, Dowlatabadi R, Weljie AM, Vogel HJ. 2009. Quantitative analysis of metabolite concentrations in human urine samples using ¹³C[1H] NMR spectroscopy. *Metabolomics* 5:307–317. <https://doi.org/10.1007/s11306-009-0155-5>.
41. Bouatra S, Aziat F, Mandal R, Guo AC, Wilson MR, Knox C, Bjorn Dahl TC, Krishnamurthy R, Saleem F, Liu P, Dame ZT, Poelzer J, Huynh J, Yallou FS, Psychogios N, Dong E, Bogumil R, Roehring C, Wishart DS. 2013. The human urine metabolome. *PLoS One* 8:e73076. <https://doi.org/10.1371/journal.pone.0073076>.
42. Corrigan RM, Bowman L, Willis AR, Kaever V, Grundling A. 2015. Cross-talk between two nucleotide-signaling pathways in *Staphylococcus aureus*. *J Biol Chem* 290:5826–5839. <https://doi.org/10.1074/jbc.M114.598300>.
43. Dengler V, McCallum N, Kiefer P, Christen P, Patrignani A, Vorholt JA, Berger-Bächi B, Senn MM. 2013. Mutation in the c-di-AMP cyclase *dacA* affects fitness and resistance of methicillin resistant *Staphylococcus aureus*. *PLoS One* 8:e73512. <https://doi.org/10.1371/journal.pone.0073512>.
44. Smith WM, Pham TH, Lei L, Dou J, Soomro AH, Beatson SA, Dykes GA, Turner MS. 2012. Heat resistance and salt hypersensitivity in *Lactococcus lactis* due to spontaneous mutation of *llmg_1816* (*gdpP*) induced by high-temperature growth. *Appl Environ Microbiol* 78:7753–7759. <https://doi.org/10.1128/AEM.02316-12>.
45. Huynh TN, Choi PH, Sureka K, Ledvina HE, Campillo J, Tong L, Woodward JJ. 2016. Cyclic di-AMP targets the cystathionine beta-synthase domain of the osmolyte transporter OpuC. *Mol Microbiol* 102:233–243. <https://doi.org/10.1111/mmi.13456>.
46. Banerjee R, Gretes M, Harlem C, Basuino L, Chambers HF. 2010. A *mecA*-negative strain of methicillin-resistant *Staphylococcus aureus* with high-level beta-lactam resistance contains mutations in three genes. *Antimicrob Agents Chemother* 54:4900–4902. <https://doi.org/10.1128/AAC.00594-10>.
47. Pugh SY, Knowles CJ. 1982. Growth of *Streptococcus faecalis* var. *zymogenes* on glycerol: the effect of aerobic and anaerobic growth in the presence and absence of haematin on enzyme synthesis. *J Gen Microbiol* 128:1009–1017. <https://doi.org/10.1099/00221287-128-5-1009>.
48. Johnson JL, Hainline BE, Rajagopalan KV. 1980. Characterization of the molybdenum cofactor of sulfite oxidase, xanthine oxidase, and nitrate reductase. Identification of a pteridine as a structural component. *J Biol Chem* 255:1783–1786.
49. Schwarz G, Mendel RR, Ribbe MW. 2009. Molybdenum cofactors, enzymes and pathways. *Nature* 460:839–847. <https://doi.org/10.1038/nature08302>.
50. Leimkuhler S, Wuebbens MM, Rajagopalan KV. 2011. The history of the discovery of the molybdenum cofactor and novel aspects of its biosynthesis in bacteria. *Coord Chem Rev* 255:1129–1144. <https://doi.org/10.1016/j.ccr.2010.12.003>.

51. Johnson JL, Rajagopalan KV. 1982. Structural and metabolic relationship between the molybdenum cofactor and urothione. *Proc Natl Acad Sci U S A* 79:6856–6860. <https://doi.org/10.1073/pnas.79.22.6856>.
52. National Research Council. 2011. Guide for the care and use of laboratory animals, 8th ed. National Academies Press, Washington, DC.
53. Colomer-Winter C, Lemos JA, Flores-Mireles AL. 2019. Biofilm assays on fibrinogen-coated silicone catheters and 96-well polystyrene plates. *Bio Protoc* 9:e3196. <https://doi.org/10.21769/BioProtoc.3196>.
54. Abranches J, Candella MM, Wen ZT, Baker HV, Burne RA. 2006. Different roles of EIIABMan and EIIGlc in regulation of energy metabolism, biofilm development, and competence in *Streptococcus mutans*. *J Bacteriol* 188:3748–3756. <https://doi.org/10.1128/JB.00169-06>.
55. Kajfasz JK, Ganguly T, Hardin EL, Abranches J, Lemos JA. 2017. Transcriptome responses of *Streptococcus mutans* to peroxide stress: identification of novel antioxidant pathways regulated by Spx. *Sci Rep* 7:16018. <https://doi.org/10.1038/s41598-017-16367-5>.